e1-6 Proton Fiducial Cuts

M. Ungaro, K. Joo

August 14, 2023

Abstract

This document describes the identification and removal of CLAS regions of low/zero efficiency and of border effects not reproducible by GSIM.

Contents

1 Fiducial Cuts **2**
1.1 Introduction . . . 2
1.2 Traditional cuts on the electron lab coordinates ϕ, θ, p . . . 2
1.3 θ versus momentum cuts . . . 4
1.4 Cuts on detectors coordinates . . . 4
1.4.1 Detectors inefficiencies . . . 8
1.4.2 Comparison with the traditional cuts . . . 8

APPENDICES
.1 Fiducial cut tent function . . . 12

1 Fiducial Cuts

1.1 Introduction

A fiducial cut on electrons is introduced to constrain regions of phase space where the CLAS response peaks at its maximum and remains rather smooth. Furthermore, some detector inefficiencies are not perfectly reproduced with GSIM and need to be removed with dedicated cuts.

Traditionally, the fiducial regions are defined in the lab coordinates of the electron reconstructed ϕ, θ, p. However, it is more natural to define the fiducial regions in the detector coordinates, because the inefficiencies are caused by tracks near their borders or hardware problems.

Since the former approach has been used in several published CLAS papers, we will keep it both as a reference and for comparison with the new approach.

1.2 Traditional cuts on the electron lab coordinates ϕ, θ, p

The fiducial cut in the lab coordinates has been determined during the π^0 analysis in the $\Delta(1232)$ region [1].

Unlike the electron case, the ϕ boundaries are asymmetric, as shown in Fig. 1.

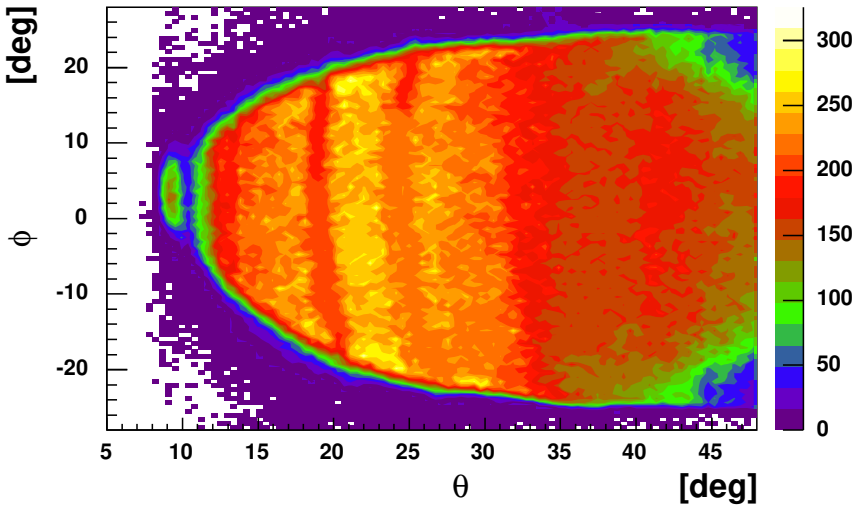

Figure 1: ϕ versus θ for sector 5. The momentum ranges from 0.9 to 1.6 GeV. The distribution is ϕ-asymmetric. Depletions along ϕ similar to the electron case are visible.

In order to evaluate ϕ boundaries the momentum has been divided into momentum and θ bins, and the distributions were fitted with the tent function shown in appendix .1. An example of such fit is shown in Fig. **??**.

The parameters are fitted as a function of θ with a fourth order polynomial:

$$\phi_{MIN} = a_0 + a_1\theta + a_2\theta^2 + a_3\theta^3 + a_4\theta^4$$
$$\phi_{MAX} = b_0 + b_1\theta + b_2\theta^2 + b_3\theta^3 + b_4\theta^4$$

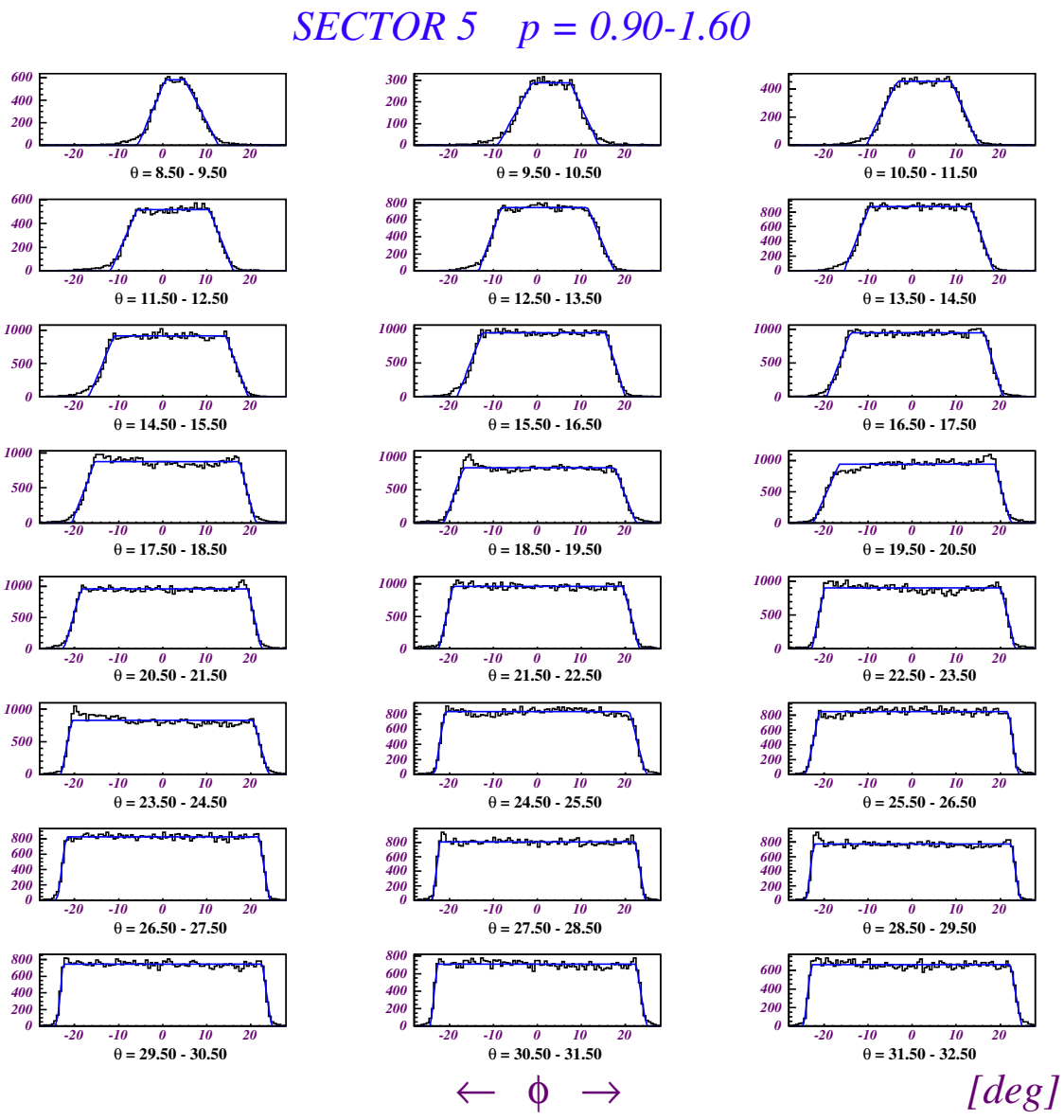

Figure 2: Trapezoid fit for sector 5. The limits of the flat ϕ region of each fit will determine the fiducial cut.

Fig. 3 shows the calculated ϕ_{MIN} and ϕ_{MAX} and the resulting fit for sector 5 and momentum range 0.9 to 1.6 GeV.

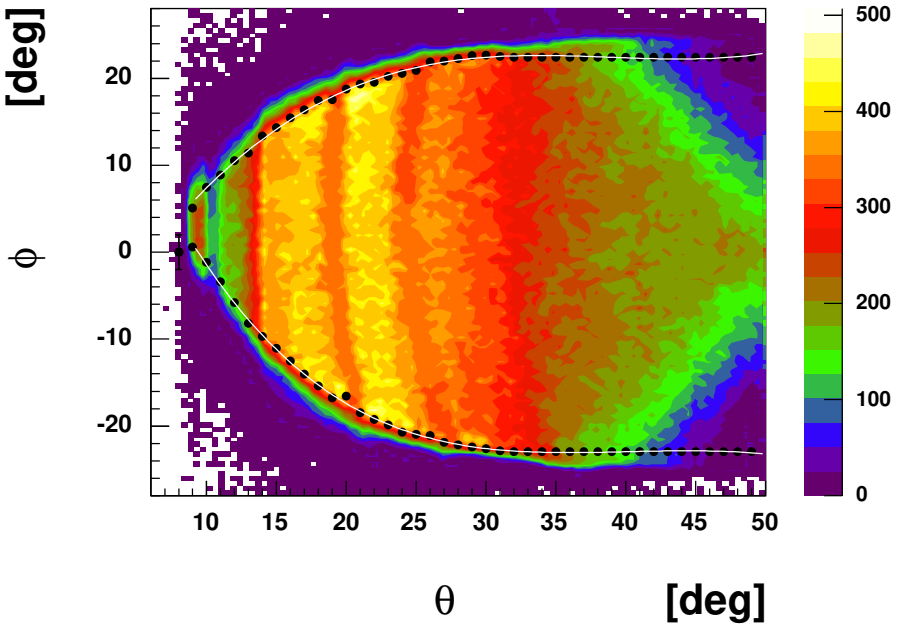

Figure 3: Result of the trapezoid fit for sector 5. The proton momentum ranges from 0.9 to 1.6 GeV. The black points are the parameters p_1 (negative ϕ) and p_2 (positive ϕ) for each θ slice considered as shown in Fig. 2. The white line is a fourth order polynomial fit to the black points.

1.3 θ versus momentum cuts

Sector 2, 3, 5 and 6 present holes and depletions which are taken care of with the cuts shown on Fig. 4 where θ is plotted against the momentum p.

The effect of the fiducial cut on sector 5 is shown in Fig. 5.

1.4 Cuts on detectors coordinates

As the electrons swim through the detectors, they are subject to inefficiencies near the sector edges. This applies to the 3 regions of the drift chambers (DC1, DC2, DC3) and the time of flight detector plane (SC). An edge cut for the calorimeter was already applied in the electron ID.

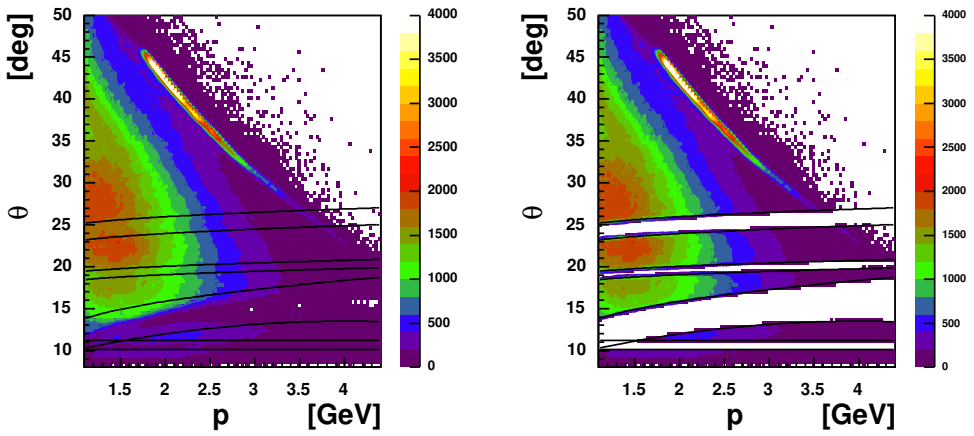

Figure 4: θ versus p for protons sector 5. A depletion is clearly visible and cut out.

The X vs Y distributions of the electron tracks in the DCs and the SC planes in sector 1 are shown in Fig. 6. This section describes the algorithm used to select thigh occupancy regions edges.

In each sector and each plane, 12 bins in X are defined; in each bin, the Y distribution is fitted with a "tent" function $t(y)$ (defined in appendix .1) to select the high efficiency edges. An example of such fit is show in Fig. 7 for sector 1 in the DC3 plane, for 4 bins in X. The fit cleanly identifies the steep rises and falls of the distributions and the relatively flat regions in between.

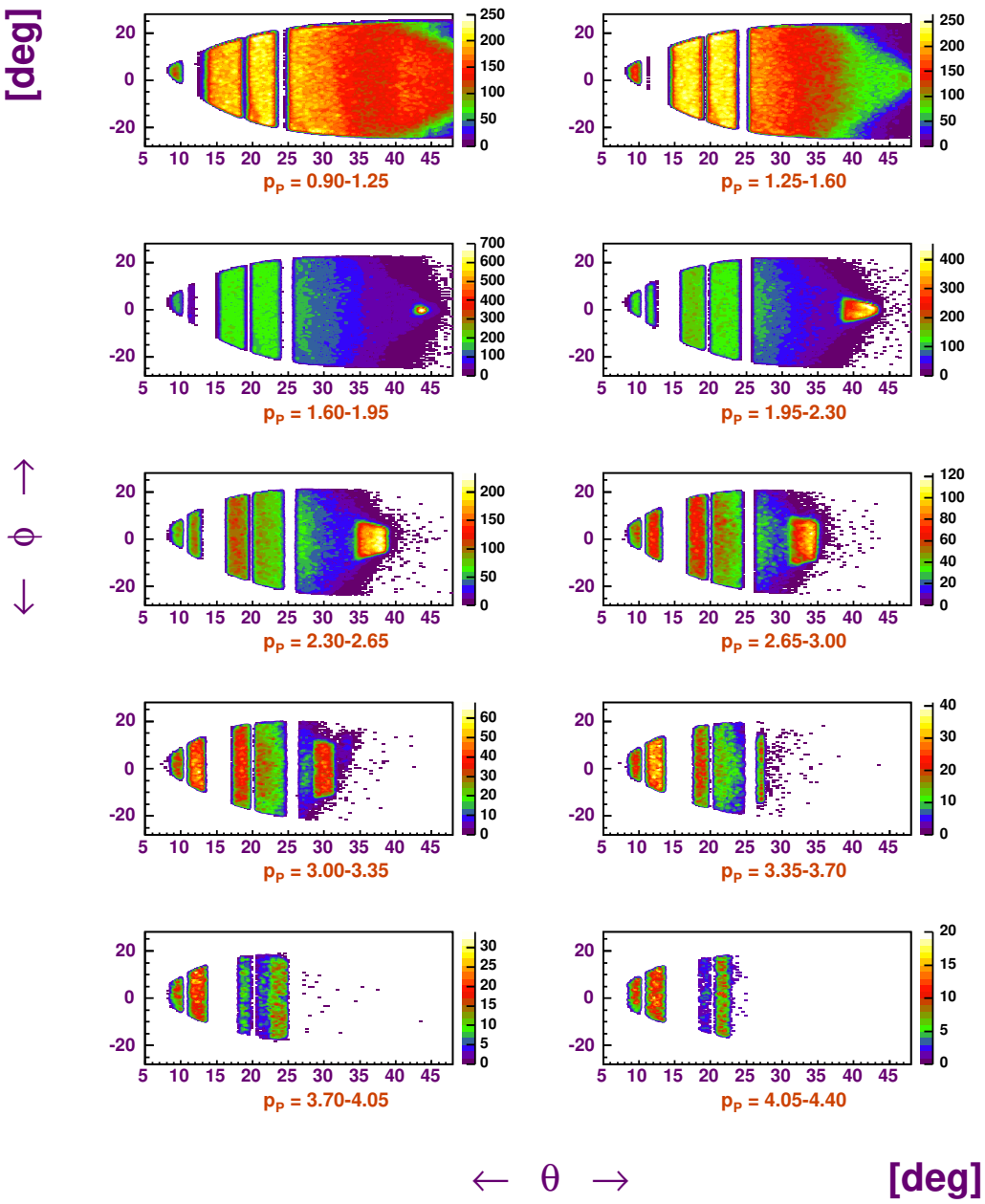

Figure 5: Sector 5 ϕ versus θ after fiducial cut. The empty bands in this sector are unfortunate because the forward ones occur where many protons of interest to us are expected.

Figure 6: The X vs Y distribution of the tracks in the drift chambers and the time of flight detector plane (SC) for sector 1. The edges selection algoritm described in the text resulted in the black lines, which are the fit of the Y distributions for each X bin.

Figure 7: Y distribution for 4 X bins in the DC3 plane for sector 1. The black lines are the tent fit of the Y distributions. The result of the first is the two points of intersection between the straight lines (steep rise) and the parabole fit (flat region). The two points are then plotted in the XY plane and fitted with a parabola, see for example Fig. 6 and **??**.

The results of the tent fit are the two points of intersection between the straight lines (steep rise) and the parabole fit (flat region). The two points are then plotted in the XY plane for all the X bins and fitted with a parabola, see for example Fig. 8.

This procedure results in a fiducial cut function for each plane and each sector.

1.4.1 Detectors inefficiencies

The detector coordinates plots allow to correlate hardware inefficiencies with depletions in the XY distributions. For example, in the DC planes, where neighboring group of wires are powered by the same HV supply and axial and stereo wires are tilted by 6^0 with respect to each other, the inefficiencies will appear as:

- Axial wires: horizontal bands in the XY distributions
- Stereo wires: 6^0 tilted bands in the XY distributions

Three examples of such hardware problems are summarized in Fig. 8. These regions are removed with dedicated cuts represented by straight lines in the XY plane, horizontal for the axial wires and 6^0 tilted for the stereo wires.

Figure 8: The X vs Y distribution of the electron tracks intersection wiht the DC2 (left) and DC1 (right) planes in sector 5. The left distributions shows one depletion for the stereo wires, while the right distribution shows two depletions for the axial wires.

1.4.2 Comparison with the traditional cuts

The effect of the fiducial and inefficiencies cuts are compared with the traditional ϕ, θ, p cuts. The comparison highlights the advantages of the new approach:

- identify the real edge effects in the detector
- hardware problems are represented by straight lines in the XY plane
- no momentum dependence of the cuts

This comparison is shown as an example for sector 5 and a momentum bin in Fig. 9. The before and after ϕ vs θ distributions in sector 5 for all the momentum bin are shown in Fig. **??** and **??** respectively.

The complete set of plots is available in appendix **??**.

Figure 9: Comparison between the traditional cuts (function of ϕ, θ, p) and the new cuts on the XY detector coordinates. Top left: ϕ vs θ before any cuts. Top right: ϕ vs θ after the XY cuts cuts. The traditional cuts superimposed and shown with black lines. Notice that the traditional cuts would remove events at very small θ and large ϕ, due to its functional form. Bottom left: DC1 plane after the fidu XY cuts. Bottm right: DC2 plane after the fidu XY cuts. Notice how the DC1 axial wires depletion is reflected in the DC2 plane. This reflection moves depending on the momentum bin and would be hard to model using the traditional cuts.

Figure 10: ϕ vs θ distributions in sector 5 for all the momentum bin before the XY fiducial cuts.

Figure 11: ϕ vs θ distributions in sector 5 for all the momentum bin after the XY fiducial cuts.

References

[1] M.Ungaro, *Single π^0 elctroproduction from $\Delta(1232)$ at high momentum transferred with CLAS*

[2] M.Ungaro, *Proton fiducial cut for single π^0 elctroproduction in the first and second resonance regions*

M. Ungaro, K. Joo

.1 Fiducial cut tent function

```
double tent(double *X, double *par) {
    double x = X[0];

    double p0 = par[0];
    double p1 = par[1];
    double p2 = par[2];
    double p3 = par[3];
    double p4 = par[4];
    double a  = par[5];

    // parabola parameters
    // y = ax2 + bx + c
    // a = par[5]
    // with two constrains given by the two points at x,y = (p1, p4), (p2, p4):
    double b = -a * (p1 * p1 - p2 * p2) / (p1 - p2);
    double c = p4 - a * p1 * p1 - b * p1;

    if (x < p1 - p0) return 0;                                        // no signal
    if (x >= p1 - p0 && x < p1) return (p4 / p0) * (x - p1 + p0);     // steep rise
    if (x >= p1 && x < p2) return a * x * x + b * x + c;              // parabola
    if (x >= p2 && x < p2 + p3) return (p4 / p3) * (-x + p2 + p3);    // steep descend
    if (x >= p2 + p3) return 0;                                       // no signal

    return 0;
}
```

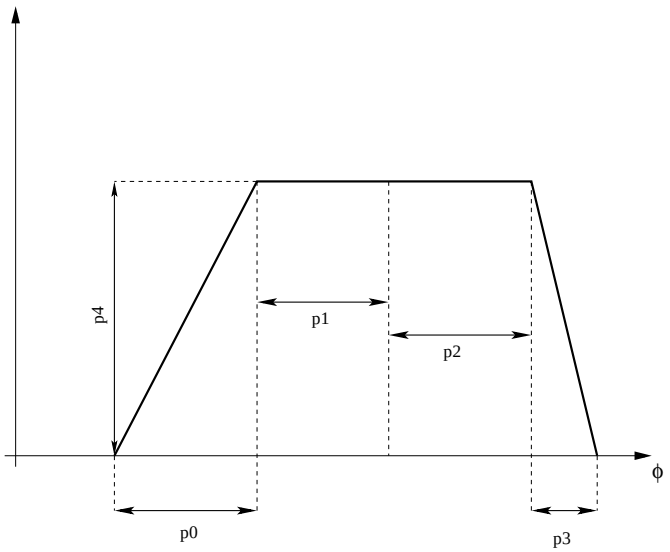

Figure 12: The trapezoid function used for the ϕ fit. The parameters p_1 and p_2 determine the fiducial cut lower and upper limits.

The trapezoid fit gives the parameters p_1 and p_2 described above for each θ considered in each momentum bin.